Random Particle Model for Fracture of Aggregate or Fiber Composites

By Zdeněk P. Bažant,[1] Fellow, ASCE, Mazen R. Tabbara,[2] Student Member, ASCE, Mohammad T. Kazemi,[3] and Gilles Pijaudier-Cabot,[4] Associate Member, ASCE

Abstract: A particle model for brittle aggregate composite materials such as concretes, rocks, or ceramics is presented. The model is also applicable to the behavior of unidirectionally reinforced fiber composites in the transverse plane. A method of random computer generation of the particle system meeting the prescribed particle size distribution is developed. The particles are assumed to be elastic and have only axial interactions, as in a truss. The interparticle contact layers of the matrix are described by a softening stress-strain relation corresponding to a prescribed microscopic interparticle fracture energy. Both two- and three-dimensional versions of the model are easy to program, but the latter poses, at present, forbidding demands for computer time. The model is shown to simulate realistically the spread of cracking and its localization. Furthermore, the model exhibits a size effect on: (1) The nominal strength, agreeing with the previously proposed size effect law; and (2) the slope of the post peak load-deflection diagrams of specimens of different sizes. For direct tensile specimens, the model predicts development of asymmetric response after the peak load.

Introduction

It is now generally accepted that inelastic deformation and fracture of brittle heterogeneous materials such as concrete or fiber composites can be adequately modeled neither by classical (local) continuum material models nor by linear elastic fracture mechanics. Although nonlinear fracture models and nonlocal continuum models can no doubt go a long way towards a realistic description, they are inherently incapable of capturing those phenomena which are strongly affected by the randomness of material heterogeneity on the microscale and are localized to a small but non-negligible region. The continuum models can describe well the mean of the macroscopic material response but not its variance. Even when generalizations such as the stochastic finite element method are considered, the assumed spatial randomness can only be correct in the overall sense and cannot capture the effect of random local material inhomogeneities on the localization of damage and failure. It is for these reasons that a direct simulation of the random microstructure of these materials is useful. As demonstrated by Zubelewicz and Bažant (1987), a model simulating the microstructure can describe progressive distributed microcracking with gradual softening and with a large cracking zone (large relative to the aggregate size).

The principal objective of the present investigation is to study the effect of the size of the specimen or structure on the maximum load, the subsequent softening behavior, and the spread of the microcracking zone. These are the key questions of fracture modeling. We will model the material as a system of randomly configured circular particles. This model is intended to simulate the behavior of concrete, but can also be used for the behavior of unidirectional reinforced fiber composites in the transverse plane, with microcracks parallel to the fibers and spreading in the transverse direction.

The model we will introduce will be a modification and refinement of that recently developed by Zubelewicz and Bažant (1987). The idea of particle simulation is an older one; it was proposed by Cundall (1971), Serrano and Rodriguez-Ortiz (1973), Rodriguez-Ortiz (1974), and Kawai (1980). These works dealt with rigid particles that interact by friction and simulate the behavior of granular solids such as sand. This approach was developed and extensively applied by Cundall (1978) and Cundall and Strack (1979), who called it the distinct element method. An extension of Cundall's method to the study of microstructure and crack growth in geomaterials with finite interfacial tensile strength was introduced by Zubelewicz (1980, 1983), Zubelewicz and Mróz (1983), and Plesha and Aifantis (1983).

In this model we neglect the shear and bending interaction of neighboring particles throughout their contact layers. With such a simplification the present model becomes similar to the random truss model of Burt and Dougill (1977). These investigators verified that the random truss (or random network) yields a realistic strain-softening curve, but they did not study the fracture mechanics nor the size effect aspects. Furthermore, their method of system generation was not based on the idea of particles with a prescribed gradation.

Simplified Interaction among Particles

Two adjacent circular or spherical particles i and j [Fig. 1(*a*)] are assumed to interact only in the axial direction (i.e., shear and moment interactions in the contact zone are neglected). As a generalization of the previous model by Zubelewicz and Bažant (1987), the particles are assumed to be elastic rather than rigid, characterized by elastic modulus E_a. The particles are embedded in a softer matrix representing the portland cement paste in the case of concrete, or a polymer in the case of various fiber composites. The matrix is initially elastic, characterized by elastic modulus E_m. The stiffness of the connection between particles i and j is approximated as

$$S = (S_i^{-1} + S_m^{-1} + S_j^{-1})^{-1} \quad \ldots\ldots (1)$$

in which

$$S_i = \frac{E_a A_i}{L_i}; \qquad S_m = \frac{E_m A_m}{L_m}; \qquad S_j = \frac{E_a A_j}{L_j} \quad \ldots\ldots (2)$$

$$L_i = \gamma r_i; \qquad L_j = \gamma r_j; \qquad L_m = L - L_i - L_j \quad \ldots\ldots (3)$$

where r_i and r_j = the radii of particles i and j; L = the distance of their

[1]Walter P. Murphy Prof. of Civ. Engrg., Ctr. for Advanced Cement-Based Matls., Northwestern Univ., Evanston, IL 60208.

[2]Grad. Res. Asst., Ctr. for Advanced Cement-Based Matls., Northwestern Univ., Evanston, IL.

[3]Grad. Res. Asst., Ctr. for Advanced Cement-Based Matls., Northwestern Univ., Evanston, IL.

[4]Sci., Laboratoire de Mécanique et Technologie, Ecole Normale Supérieure, Cachan, /CNRS/ Univ. Paris 6 France; formerly, Grad. Res. Asst., Northwestern Univ., Evanston, IL.

Note. Discussion open until January 1, 1991. To extend the closing date one month, a written request must be filed with the ASCE Manager of Journals. The manuscript for this paper was submitted for review and possible publication on August 21, 1989. This paper is part of the ***Journal of Engineering Mechanics***, Vol. 116, No. 8, August, 1990. ©ASCE, ISSN 0733-9399/90/0008-1686/$1.00 + $.15 per page. Paper No. 24923.

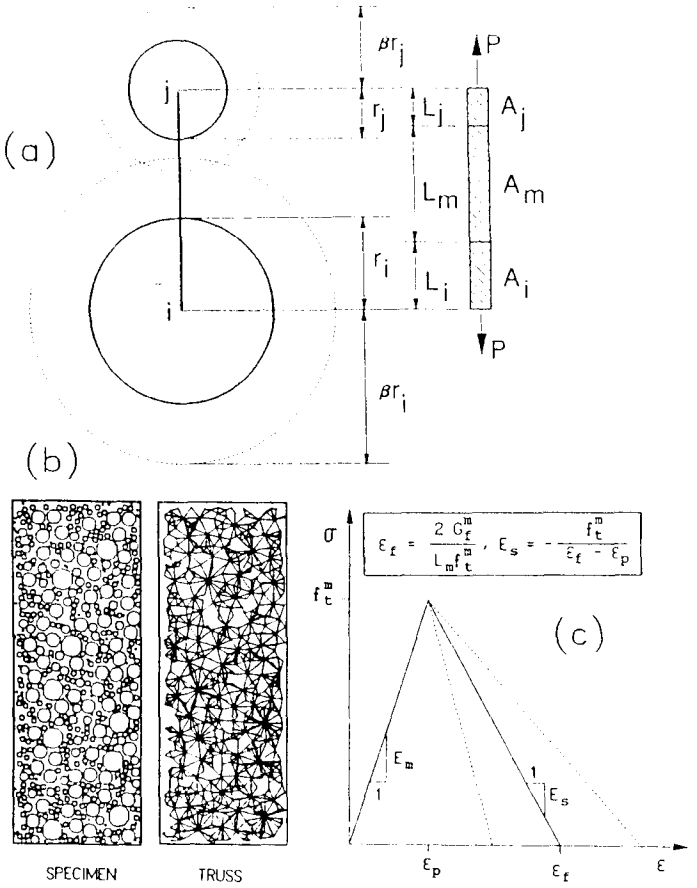

FIG. 1. (*a*) Two Adjacent Circular Particles with Radii r_i and r_j and Corresponding Truss Member ij; (*b*) Typical Randomly Generated Specimen and Its Corresponding Mesh of Truss Elements; (*c*) Constitutive Law for Matrix

centers, and the interaction is assumed to correspond to a strut [Fig. 1(*a*)] whose length is subdivided into segments L_i, L_j, and L_m representing the particles and the interparticle contact layer of matrix. The lengths of these segments are determined by an empirical factor γ, for which the value $\gamma = 0.9$ has been used. A_i, A_j, and A_m are the cross section areas of the strut segments describing the particles and the matrix; they are defined for the two-dimensional case of circles as

$$A_i = A_j = A_m = 2 \min (r_i, r_j) \quad \ldots\ldots (4a)$$

and for the three-dimensional case of spheres as

$$A_i = A_j = A_m = \pi \min (r_i^2, r_j^2) \quad \ldots\ldots (4b)$$

The strut segment L_m, representing the interparticle contact region of the

matrix, is assumed to exhibit softening characterized by the triangular stress-strain relation in Fig. 1(*c*). The softening behavior, which starts after reaching a certain specified strain ϵ_p for the peak stress, is determined by the fracture energy G_f^m of the interparticle layer (matrix and interface of matrix and particle) and is assumed to be a material constant. The fracture energy is equal to the area under the stress-strain diagram times length L_m (the fracture may, of course, localize, but strain ϵ is defined as the average strain over length L_m, not as some local strain). Thus $G_f^m = L_m f_t^m \epsilon_f / 2$, with $f_t^m = E_m \epsilon_p$ = strut strength. From this, the strain at the end of softening (at which complete interfacial crack forms) is

$$\epsilon_f = \frac{2G_f^m}{L_m f_t^m} \quad \ldots\ldots (5)$$

In the numerical simulation that follows, the values used are such that $\epsilon_f > \epsilon_p$ even for the largest particle separations considered. However, for a small fracture energy or for interactions between particles that are sufficiently far apart, it could happen that $\epsilon_f < \epsilon_v$, which would mean that the response would exhibit a snapback instability. Although this would represent a complication for the numerical solution, it could be handled with minor modification.

The tangential softening modulus E_s [Fig. 1(*c*)] is defined by the relation $E_s(\epsilon_f - \epsilon_p) = -f_t^m$, from which

$$E_s = -\frac{f_t^m}{\epsilon_f - \epsilon_p} \quad \ldots\ldots (6)$$

If the length L_m is varied, the softening modulus E_s changes as shown by the dotted line in Fig. 1(*c*), so as to preserve a constant value of G_f^m. In the case of unloading, the matrix material is assumed to follow a straight line parallel to the initial tangent. On reloading, this line is retraced up to the virgin stress-strain diagram, which is then followed at further increase of strain.

Let $\bar{u}_i$, $\bar{u}_j$ be the displacements at the ends of segment L_m in the direction ij. The strain in the matrix is

$$\epsilon = \frac{\bar{u}_j - \bar{u}_i}{L_m} \quad \ldots\ldots (7)$$

Introducing the displacements u_i and u_j at particle centers i and j (nodes) in the direction ij, we have

$$\bar{u}_i = u_i + \frac{P}{S_i}; \qquad \bar{u}_j = u_j - \frac{P}{S_j} \quad \ldots\ldots (8)$$

Substituting in Eq. 7, we get

$$\epsilon = \frac{1}{L_m}\left(u_j - u_i - \frac{P}{S_j} - \frac{P}{S_i}\right) \quad \ldots\ldots (9)$$

in which P = the interparticle force. The strain given by Eq. 9 and its previous history makes it possible to calculate the stress in the strut according to the stress-strain relation for loading and unloading in the segment L_m.

Having neglected shear and moment interactions among particles, the particle system is equivalent to a pin-jointed truss and can be treated as a special case of a finite element system. The static response of the particle system to the prescribed loading is calculated in small displacement increments, in each of which the behavior of the connecting strut is described according to Eqs. 1–9. These equations are used to formulate the stiffness matrix of each connecting strut in the global coordinates, and these stiffnesses are assembled in each loading step into the structural stiffness matrix.

As an alternative, one can use the secant stiffness iteration (Owen and Hinton 1980), which is based on the total force-displacement relations for the connecting struts. The solution algorithm proceeds in this case in the same manner as described for layered beam finite elements in Bažant et al. (1987).

The formulation just outlined represents a simplification of the actual behavior on the microscale. The detailed growth of microcracks on a scale smaller than the aggregate sizes (i.e., the scale of grains in the matrix) is not modeled. Furthermore, the three-dimensional nonlinear constitutive properties of the particle and matrix material are not taken into account. In this regard, however, we must realize that the physics of macroscopic phenomena generally depends only on the principal phenomena on the microscale. It is insensitive to various detailed phenomena and processes on the microscale, which tend to average out or cancel each other. Based on this experience, the description of the microscopic phenomena should always be greatly simplified if the purpose is a macroscopic model, but the simplification must be a realistic one. It seems that the present model might be adequate in this spirit.

Random Generation of Particle Configuration

An important aspect of the simulation is the generation of the random geometrical configurations of the particles, which satisfies the basic statistical characteristics of the real material, such as concrete. The random configuration must be macroscopically homogeneous in space and macroscopically isotropic. The configuration must meet the required granulometric distribution of the particles of various sizes, as prescribed for the mix of concrete. The problem of random generation of the configurations with such constraints has various difficult and sophisticated aspects. These are for example discussed by Plesha and Aifantis (1983), who also review various pertinent mathematical theories.

After experimenting with various alternatives, the following simple procedure of random generation has been adopted.

1. The volume ratio for each particle size is specified in advance.
2. Using a random number generator from a standard computer library, generate the pairs of coordinates (x_i, y_i), $i = 1, 2, \ldots$, of the particle centers (or coordinate triplets, in 3-D), one pair after another, assuming a uniform probability distribution for these points throughout the specimen. This is particularly easy for specimens with rectangular boundaries, for which the probability distribution of each coordinate is independent and uniform over a line segment, and equally easy for specimens that can be subdivided in a finite number of identical elements (e.g., squares or cubes).
3. For each generated coordinate pair (or triplet), check for possible overlaps of the new particle with the previously placed particles and with the specimen boundaries. Reject the coordinate pair if an overlap occurs.
4. Random generation of the coordinate pairs proceeds until the last particle of the largest size has been placed within the specimen. Then the entire random placement process of the particles is repeated for the particles of the next smaller size, and then again for the next smaller size, until the last particle of the smallest size has been placed within the specimen.

A different approach, which has been used, for example, by Cundall (1978), is to simulate actually the production of the material. In the case of sand, this approach tries to simulate the pouring of the sand into a form. The particles are taken one by one and dropped vertically at random locations in the horizontal plane onto the heap of the sand already deposited. After coming in contact, each particle is allowed to roll or slide to a stable position. This approach produces a dense packing, which is no doubt quite realistic for sand. However, the random particle system obtained is not isotropic. Moreover, the programming is considerably more sophisticated than that for the presently used procedure. This simulation also ignores the fact that, in a material such as concrete or a fiber-reinforced polymer, each particle is wrapped in a layer of adhering matrix, which causes perfect contacts to be less likely than particle locations with some separation.

A salient feature of the present model is the existence of a contact layer of matrix separating the adjacent random particles. This makes it possible to model interaction between particle pairs that are not in contact. This feature has been handled in the manner previously introduced by Zubelewicz and Bažant (1987), in which each circular particle is assumed to be surrounded by a circular influence zone of a larger radius βr where r is the radius of the particle [Fig. 1(*a*)]. After some numerical experimentation, the value $\beta = 1.65$ has been adopted. The particles are assumed to interact (i.e., the connecting strut is assumed to exist) only when their influence zones overlap. When these zones do not overlap, the particles are assumed to have no interaction (i.e., no connecting strut exists). It should be noted that the use of the influence zone greatly simplifies the random generation of the particle locations and makes the aforementioned procedure possible.

There is one limitation that is caused by the hypothesis that the particle interactions are only axial. The average Poisson's ratio ν for the initial elastic deformations cannot be specified as measured in experiments but is implied by the specified characteristics of the random particle system. For a random truss representing a system of particles of one size, the value of ν for a very large number of particles asymptotically approaches 1/3 for the two-dimensional case, and 1/4 for the three-dimensional case. This is a well-known property of large macro-homogeneous lattices. When the particle sizes are unequal, the value of ν can be different, but for the present two-dimensional calculations it has been close to 1/3. This value of the Poisson's ratio is too high for concrete. To obtain a realistic value (approximately 0.18), one could include shear interactions, as in Zubelewicz and Bažant (1987), although other measures might be possible.

NUMERICAL STUDIES

Response of Unnotched Specimens

The response of various unnotched concrete specimens has been calculated and compared to what is known from testing and other analytical studies. Examples of the randomly generated particle configurations are seen in Figs. 1(*b*) and 2. Fig. 1(*b*) also shows the truss to which the particle model is equivalent.

Geometrically similar specimens of various sizes, with depths = $3d_a$, $6d_a$, and $12d_a$, where d_a = maximum particle size (12 mm), have been analyzed. The length of the specimens is always $L = 8d/3$. The diameters of the particles are 12, 8, 5, 3, and 1 mm. The volume ratio of particles for each diameter is selected to model concrete. Details of the number of particles for each size are given in Table 1.

Size Effect

A salient consequence of heterogeneity, which has fracture mechanics as well as probabilistic aspects, is the size effect on the failure load. If the failure is governed by criteria in terms of stress or strain (yield criteria), then geometrically similar specimens of different sizes must fail at the same value of the nominal stress at failure σ_N, defined as P_u/bd, where P_u = maximum load, d = depth of specimen, and b = thickness. To test this property, the specimens shown in Fig. 2 were subjected to prescribed uniform longitudinal displacement u at one end [Fig. 3(*a*)] and restrained against displacements at the opposite end. Displacement u has been incremented in small steps, and the axial force resultant P calculated for the following material properties: G_f^m = 24 N/m, f_t^m = 3 MPa, E_m = 30 GPa, and $E_a = 6E_m$. The diagrams of load P versus load-point displacement u have been constructed; they are plotted in Figs. 3(*b–d*) for the small, medium, and large specimens. Fig. 3(*e*) shows the load-deflection curves for specimens 1A, 2A, and 3A scaled so that the peak point would coincide with (1, 1). The figure reveals that the post-peak declining slope gets steeper as the specimen size increases.

The data points for maximum loads are plotted in Fig. 4 in terms of stress σ_N as a function of the specimen depth d. The nominal stress is normalized with respect to f_u, an arbitrary measure of material strength, taken here as $f_u = f_t^m$ = 3 MPa. The depth is normalized with respect to d_a, the diameter of the largest particle (12 mm). We see considerable scatter; therefore, the values of the nominal stress are averaged for each specimen size and are plotted as stars in Fig. 4. These plots clearly reveal that there is a size effect.

The size effect for materials that exhibit progressive cracking is known approximately to follow the size effect law proposed by Bažant (1984)

TABLE 1. Number of Particles in Specimens

Specimen (1)	d (mm) (2)	L (mm) (3)	Diameter (mm) 12 (4)	8 (5)	5 (6)	3 (7)	1 (8)
1A, B, C, D	36	96	2	16	14	68	35
2A, B	72	192	9	66	58	273	140
3A	144	384	39	264	235	1,095	563

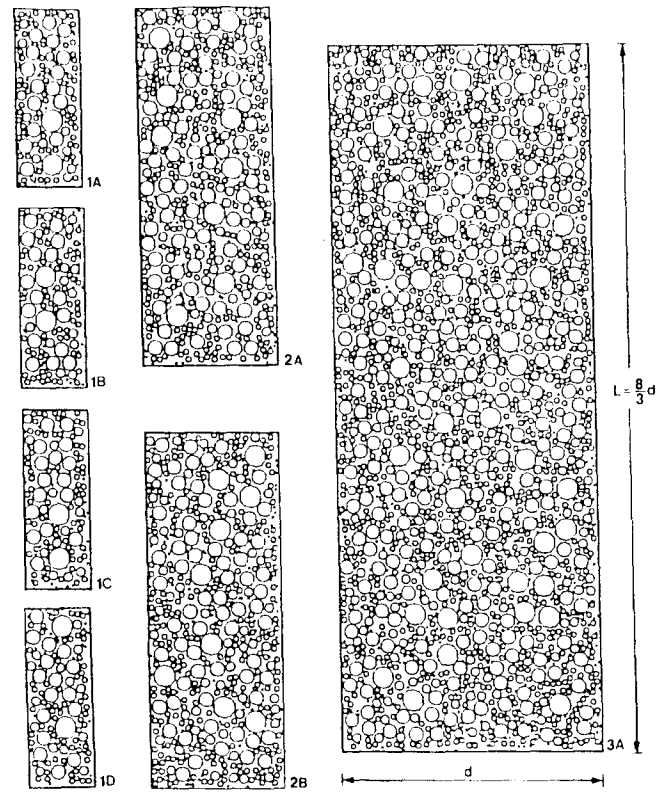

FIG. 2. Geometrically Similar Specimens of Various Sizes with Randomly Generated Particles

$$\sigma_N = \frac{Bf_u}{\sqrt{1 + \dfrac{d}{d_0}}} \qquad (10)$$

where $d_0 = \lambda_0 d_a$; and B, λ_0 = empirical parameters. This law, which is approximate but usually applicable to size ranges up to 1:20, represents a gradual transition between the strength (or yield) criterion, for which there is no size effect on nominal strength, and linear elastic fracture mechanics, for which the size effect is the strongest possible ($\sigma_N \propto d^{-1/2}$). For data fitting it is convenient to transform Eq. 10 to the linear regression plot $Y = AX + C$, in which $X = d/d_a$, $Y = (f_u\sigma_N)^2$, $C = 1/B^2$, and $A = C/\lambda_0$.

For comparison, the lines representing the size effect according to the strength (or yield) criterion and according to the linear elastic fracture mechanics are also shown in the Fig. 4(*b*). From this it is evident that the size effect obtained is intermediate between the strength criterion and the linear elastic fracture mechanics. This may be expected on the basis of the fact that the specimens do not fail at cracking initiation but only after a crack

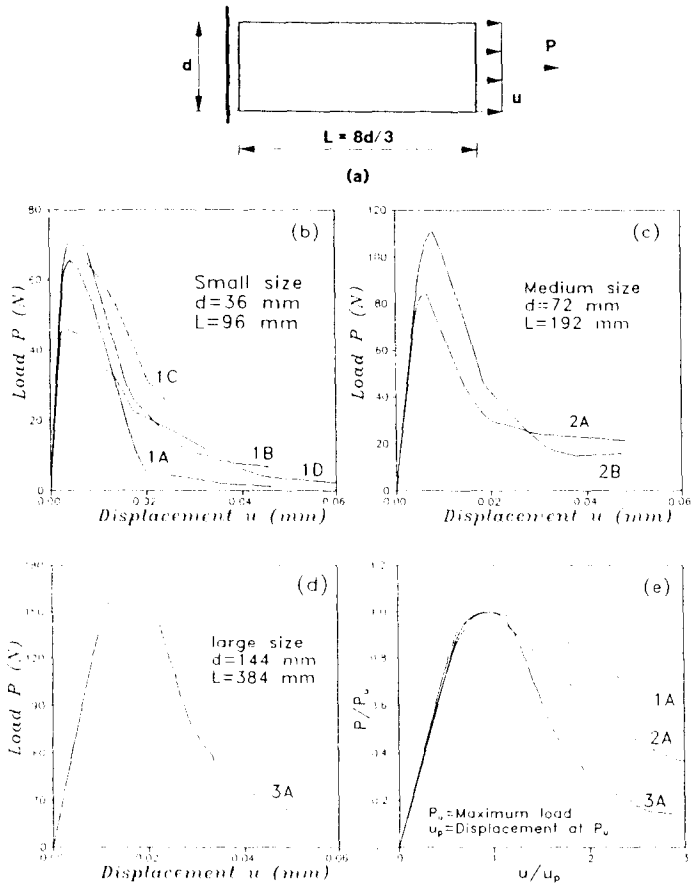

FIG. 3. (*a*) Direct Tension Specimens with d = 36, 72, and 144 mm; (*b*) Load-Displacement Curve for Small Specimen; (*c*) Load-Displacement Curve for Medium Specimen; (*d*) Load-Displacement Curve for Large Specimen; and (*e*) Normalized Load-Displacement Curves for Specimens 1A, 2A, and 3A

band has already developed, in which case nonlinear fracture mechanics should be applicable.

Progressive Spread of Cracking

Fig. 5 shows for the various specimens their microcrack patterns at the last calculated point on the load-deflection curve. Fig. 6(*c*) shows these patterns as they develop in specimen 1A at various stages of loading corresponding to points 1, 2, 3, and 4 shown in Fig. 6(*a*). The fully formed and open cracks (for which the stress is reduced to 0, $\epsilon > \epsilon_f$) are shown by the solid lines, and the partially formed, developing (active) cracks that correspond to strain-softening states are shown by the dashed lines. Also shown are the previously formed cracks that are getting unloaded [Fig. 6(*b*)]; these are represented by two stars. We see that the cracks first start at many ran-

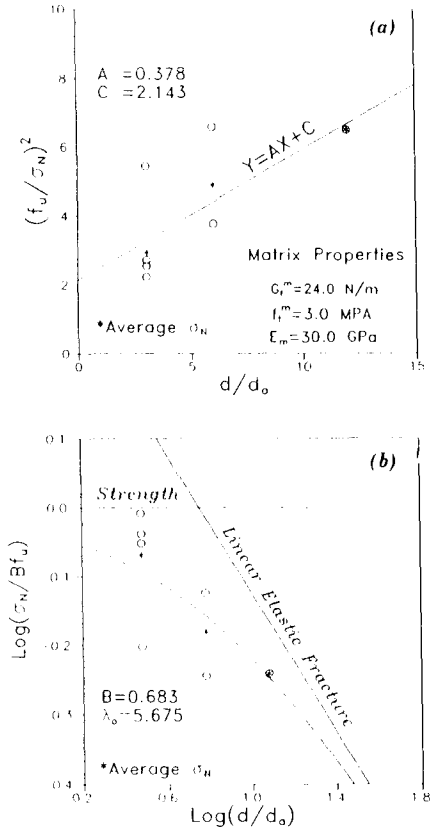

FIG. 4. (*a*) Linear Regression Plot; and (*b*) Size Effect Plot Constructed from Maximum Load Values Calculated for Direct Tension Specimens of Various Sizes

dom locations throughout the specimen, but later many of these partially formed cracks unload, and only some of them, lying in a narrow transverse band, open further and lead to the final fracture.

The unloading behavior is further documented in Fig. 7, which shows the evolution of the strain determined from the line segments 1 and 2. The first line segment always undergoes loading, crossing the developing crack band, while the second line segment undergoes partial softening but soon reverses to unloading [Fig. 7(*b*)].

Scatter of Stress Profile and Symmetry Breakdown

The distribution of the longitudinal component of the interparticle forces P_i throughout the cross section at distance x = 60 mm from the fixed end is sketched, for specimen 1A, at various stages of loading, in Fig. 8. Similar plots for specimen 3A at two locations x = 160 mm and x = 240 mm are shown in Fig. 9. We see that the nonuniformity in the distribution is getting more pronounced at later stages of loading. Furthermore, we see that the resultant of the longitudinal force tends to shift away from the center line,

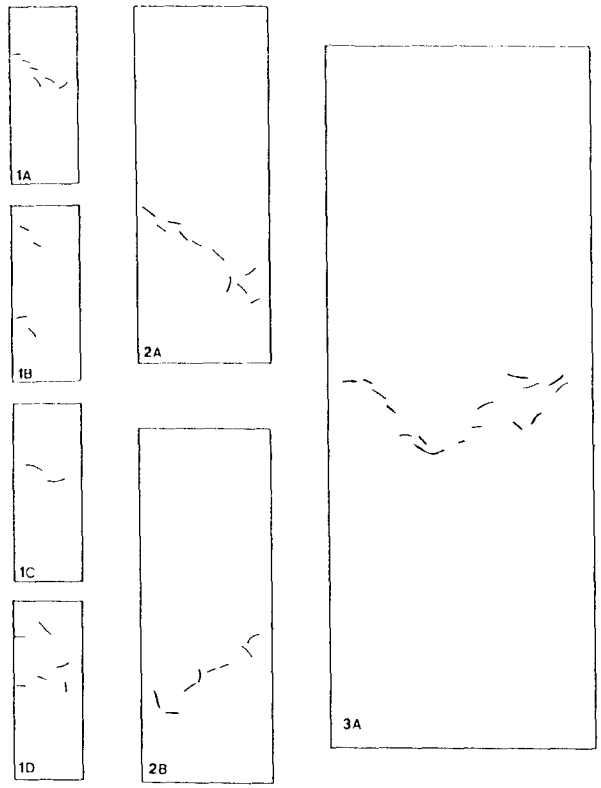

FIG. 5. Cracking Patterns at Last Calculated Point on Load-Deflection Curve for Unnotched Specimens in Tension

which indicates a tendency for these specimens to follow an asymmetric deformation pattern (a similar asymmetry is in fact indicated by analysis of the stable paths of fracture propagation). The eccentricity, e, of the force resultant, P, is plotted as a function of P for two specimens (1A and 1B) in Fig. 10, in which the tendency towards an increasing eccentricity is clearly seen. Development of such asymmetric response was observed in unnotched tensile specimens in the experiments of Bažant and Pijaudier-Cabot (1989). A similar asymmetry was seen to develop in the experiments of Rots et al. (1987).

Boundary Layer

It is also apparent from Figs. 8 and 9 that the largest longitudinal forces tend to be transmitted through the interior of the specimen, and the boundary layer on the average transmits lower forces than the interior. This is a manifestation of what is known in concrete technology as the "wall effect." The boundary layer has on the average a smaller content of the stiff particles and a higher content of the soft matrix than does the interior of the specimen. This is inevitable when the material is cast into a form. On the other hand,

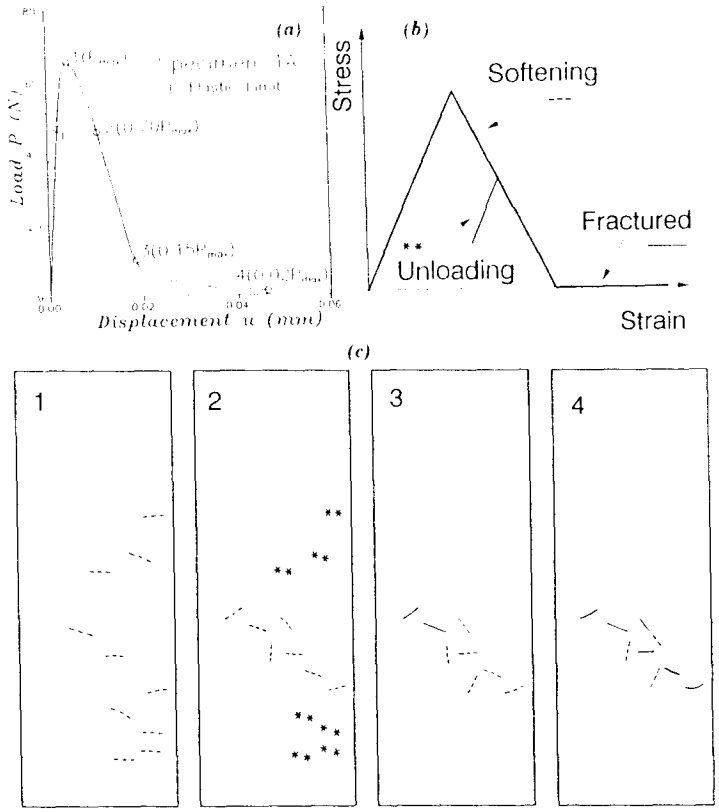

FIG. 6. (*a*) Load-Displacement Curve for Specimen 1A; (*b*) Constitutive Law for Matrix; and (*c*) Evolution of Cracking with Loading and Localization

if the specimen were cut out from a larger block of the material, then the boundary layer would have on the average exactly the same composition statistics as the interior. However, there would still be a wall effect, although probably a much smaller one, because transverse stresses are transmitted across longitudinal straight lines in the interior, while transmission of the transverse stresses is interrupted at the surface.

Macroscopic Poisson's Ratio

To determine the Young's elastic modulus E and the Poisson's ratio of the equivalent (smeared, homogenized) elastic continuum, the large specimen 3A was loaded in uniaxial tension by prescribing a very small uniform longitudinal displacement ($u = 0.004$ mm) at one end and restraining the specimen against displacement at the other end. Free sliding was allowed at the ends in the transverse direction. The displacements in the longitudinal direction, u_l, and the transverse direction, u_t, are shown in Fig. 11 for the nodes with the maximum size aggregates. Furthermore, to minimize the ef-

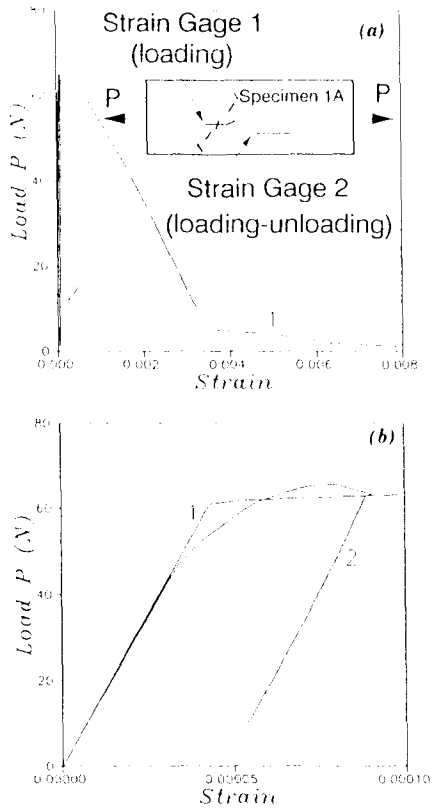

FIG. 7. Load-Strain Curves for Specimen 1A for: (*a*) Full Range of Strain; and (*b*) Small Values of Strain

fect of boundary conditions, only nodes within an interior region ($0.8d \times 0.8L$) were considered.

Fig. 11(*a*) shows for the case of mean uniaxial stress $\sigma_x = 0.39$ MPa the linear regression line for u_x as a function of the x-coordinate; its slope represents the mean (macroscopic) strain in the x-direction, $\epsilon_x = 0.1154 \times 10^{-4}$, from which $E = 33.8$ GPa. A similar regression line in Fig. 11(*b*) gives the strain in the y-direction, $\epsilon_y = -0.4234 \times 10^{-5}$. The macroscopic Poisson's ratio is then obtained as $\nu = -\epsilon_y/\epsilon_x = 0.37$. This value is close to the value of $\nu = 1/3$, which is the theoretical value for a very large two-dimensional random lattice that is statistically uniform and isotropic. Neither the calculated value $\nu = 0.37$ nor the theoretical value $\nu = 1/3$ for very large specimens is realistic for most particulate composites, including concrete, for which, typically, $\nu = 0.18$. The correct Poisson's ratio of real particulate composites cannot be attained with the truss model (random network). The reason for this limitation is that only axial interactions between the particle centers are taken into account, while shear stresses in the interparticle contact zones are neglected.

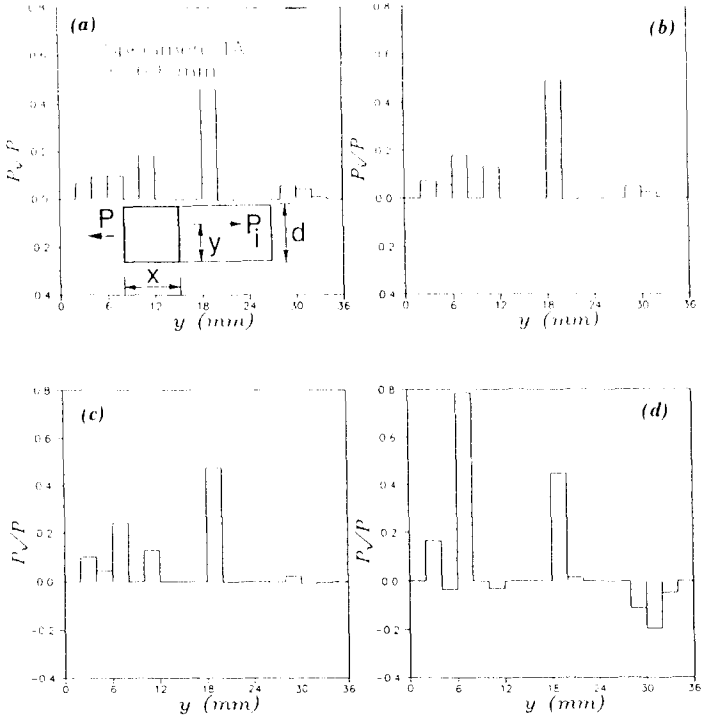

FIG. 8. Distribution of Longitudinal Component of Interparticle Forces P_i throughout Cross Section of Specimen 1A: (*a*) $P <$ Elastic Limit; (*b*) $P = P_{max}$; (*c*) $P = 0.70P_{max}$; and (*d*) $P = 0.15P_{max}$

Response of Notched Specimens

As we have seen, cracking in unnotched specimens that are initially stressed uniformly develops quite randomly. This prevents it from bringing to light fracture properties of the particle system. To see these properties, notched specimens have also been simulated with the particle model. The notches were mathematically modeled by first generating the random particle configuration as if no notch existed, and then severing all the interparticle connections that cross the line of the mathematical notch depth, $a_0 = d/6$ ($\alpha_0 = a_0/d = 1/6$).

As one basic idea of this study, it is proposed to determine the macroscopic fracture properties of the particle system by studying the size effect, since this effect represents the most important consequence of fracture mechanics. To this end, we analyze geometrically similar three-point-bend fracture specimens of three different sizes whose ratios are 1:2:4. Thus, three new specimens were generated as shown in Fig. 12.

To save computer time, the truss modeling of the random particle system covered only the central region of the beam near the notch, while the end portions of the specimen were modeled by a regular truss with linear elastic properties. This simplification has a negligible effect on the values of max-

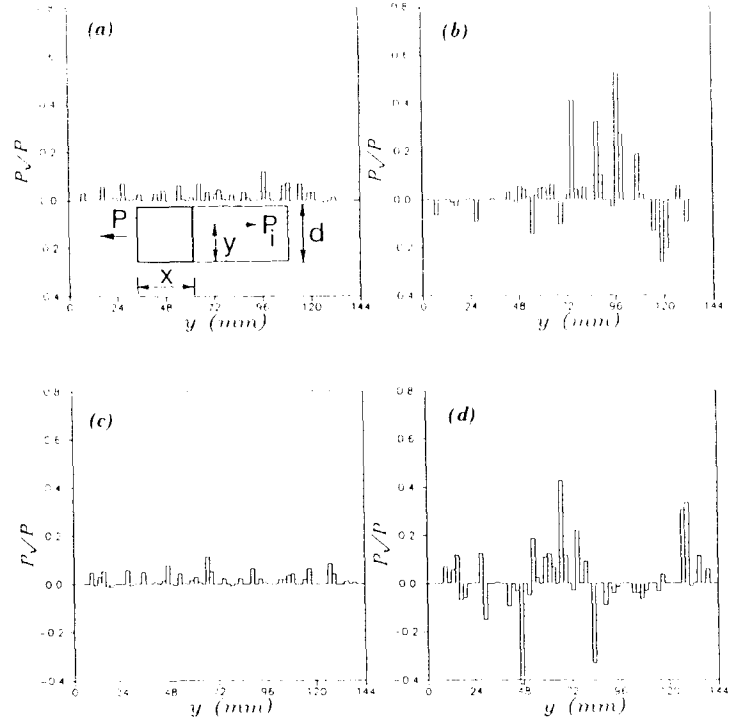

FIG. 9. Distribution of Longitudinal Component of Interparticle Forces P_i throughout Cross Section of Specimen 3A: (*a*) $P <$ Elastic Limit, $x = 160$ mm; (*b*) $P = 0.14P_{max}$, $x = 160$ mm; (*c*) $P <$ Elastic Limit, $x = 240$ mm; and (*d*) $P = 0.14P_{max}$, $x = 240$ mm

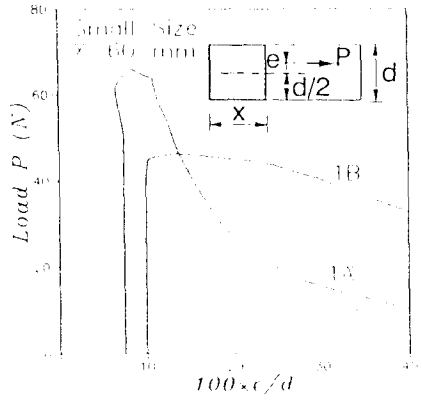

FIG. 10. Evolution of Eccentricity as Function of Load Resultant

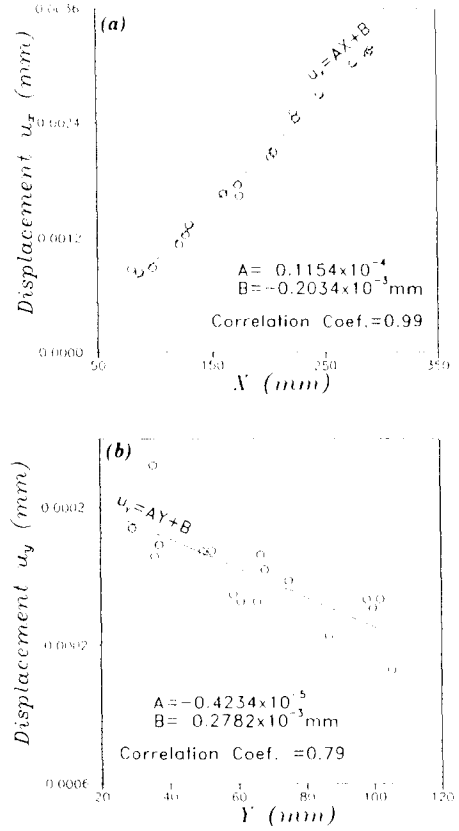

FIG. 11. Linear Regression for Components of Displacements of Nodes with Maximum Size Aggregates in: (*a*) x-Direction; and (*b*) y-Direction

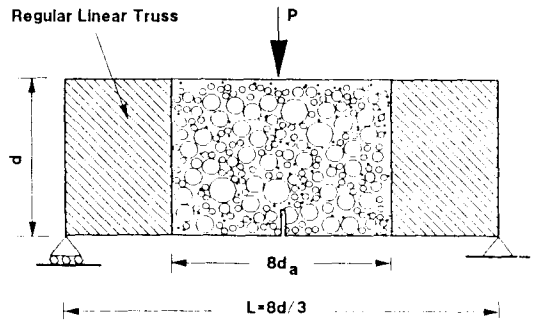

FIG. 12. Three-Point-Bend Specimens with d = 36, 72, and 144 mm

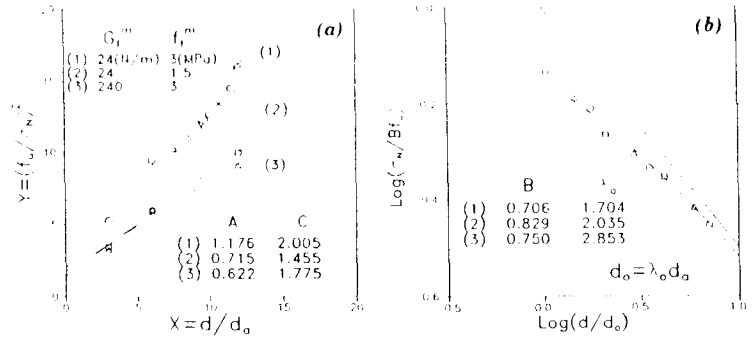

FIG. 13. (*a*) Linear Regression Plot; and (*b*) Size Effect Plot Constructed from Maximum Load Values Calculated for Three-Point-Bend Specimens of Various Sizes

imum loads, as long as all the cracking occurs only outside the regular truss and far from its boundaries. Calculations verified that this was indeed the case. For the three-point-bend specimens, the random particle region width was taken to be equal to $8d_a$ (96 mm), which coincided with the span of the smallest size specimen. Thus, no truss was added to a specimen of this size.

In the calculations of maximum loads, three different sets of matrix properties have been considered: (1) G_f^m = 24 N/m, f_t^m = 3 MPa; (2) 24 N/m, 1.5 MPa; and (3) 240 N/m, 3 MPa, with E_m = 30 GPa and $E_a = 6E_m$ for all cases. For each set, the regression line [plotted in Fig. 13(*a*)] yields the values of slope A and intercept C, from which the values of B and λ_0 follow [see Fig. 13(*b*)]. The size effect curve according to Eq. 10 is also plotted, along with all the calculated points for the different sets of matrix properties. The results show a good agreement with Eq. 10. However, for the aforementioned values of material properties, the results are closer to linear elastic fracture mechanics than the test results obtained for similar specimens by Bažant and Pfeiffer (1987).

From the size effect on maximum loads, one can determine the fracture energy G_f of the idealized material represented by the random particle system, using the formula (Bažant and Pfeiffer 1987)

$$G_f = \frac{g(\alpha_0)}{AE} f_a'^2 d_a \quad \ldots\ldots (11)$$

where E = Young's modulus (macroscopic); and $g(\alpha_0)$ = the nondimensional energy release rate according to linear elastic fracture mechanics, $g(\alpha_0)$ = 6.07 for the present specimens. On the basis of Eq. 10, one can also determine the effective size c_f of the fracture process zone according to the formula (Bažant and Kazemi 1988)

$$c_f = \frac{g(\alpha_0)}{g'(\alpha_0)} \lambda_0 d_a \quad \ldots\ldots (12)$$

where $g'(\alpha_0)$ = the derivative of $g(\alpha)$, which is evaluated at $\alpha_0 = 1/6$, and is equal to 35.2 for the present three-point-bend specimens.

Table 2 gives the values of G_f and c_f calculated for the three sets of matrix

TABLE 2. Values of Fracture Energy G_f and Process Zone Size c_f

Three-point bending (1)	Particle Model (1) (2)	(2) (3)	(3) (4)	Experiment[a] Mortar (5)	Concrete (6)
G_f (N/m)	16.5	6.8	31.2	20	37
c_f (mm)	3.5	4.2	5.9	1.9	13.5

[a]From Bažant and Kazemi (1988).

properties. Taking property set (1) as reference, the results from (2) show that a decrease of interparticle strength f_t^m will decrease G_f and increase c_f. However, results from (3) show that an increase of G_f^m will increase both G_f and c_f. Table 2 also includes the values obtained by Bažant and Kazemi (1988) from experiments on mortar and concrete. These values are in the same range as calculated here and could be matched more closely by adjusting the material properties of the model.

Numerical experience showed that the calculated maximum loads can be sensitive to the random arrangement near the notch tip and the way the notch is modeled. The length of the notch cut by a saw, which is simulated by severing the particle connection intersecting the notch, is uncertain to the extent that the notch tip can be anywhere between the last severed connection and the first unsevered connection ahead of the tip. Furthermore, one should not delete a particle whose center falls into the width of the notch cut, since this can greatly distort the results. This means that the notch cut should be considered as a line rather than an actual cut of finite width.

Conclusions

1. Random generation of a particle system with a given particle size distribution can be accomplished quite easily, because the particles are circular (or spherical) and are not in contact but are separated by contact layers whose thickness is unspecified, except for a given maximum thickness value.

2. Modeling only the axial interactions of neighboring particles seems sufficient to obtain a realistic picture of the spread of cracking and fracture in concrete. The neglect of shear interactions might cause the fracture process zone to be shorter and narrower than in real concrete fracture specimens. However, the length of this zone can be increased by increasing the value of the interparticle fracture energy (G_f^m) or by decreasing the value of the interparticle strength (f_t^m).

3. The model can describe realistically the post-peak declining load-deflection diagram, which is predicted to get steeper as the specimen size increases.

4. In contrast to local continuum models, the present model is capable of describing the size effect on the nominal strength of unnotched specimens as well as notched specimens.

5. For direct tensile specimens, the model predicts development of asymmetric response after the peak load, such that the specimen bends and the axial force resultant becomes eccentric. This agrees with laboratory tests.

6. Some improvements of the model might be appropriate in: (1) Determining the cross section areas of the truss members so as to make them dependent on

the distance between particles; (2) controlling the Poisson's ratio without having to introduce shear interaction; and (3) developing a simple method to connect the particle system in the cracking zone to a finite element mesh around this zone. Such a method would significantly reduce the number of particles needed to analyze three-dimensional or large two-dimensional problems.

Acknowledgment

Partial financial support under AFSOR contract F49620-87-C-0030DEF with Northwestern University, monitored by Dr. Spencer T. Wu, is gratefully acknowledged. Partial support for fracture studies was also received from the Center for Advanced Cement-Based Materials at Northwestern University (NSF Grant DMR-8808432). Supercomputer time on the CRAY X-MP/48 was received from the National Center for Supercomputing Applications (NCSA) under grant number MSM890006N.

Appendix. References

Bažant, Z. P. (1984). "Size effect in blunt fracture: Concrete, rock, metal." *J. Engrg. Mech.*, ASCE, 110(4), 518–535.

Bažant, Z. P., and Pfeiffer, P. A. (1987). "Determination of fracture energy from size effect and brittleness number." *ACI Matls. J.*, 84(6), 463–480.

Bažant, Z. P., Pan, J., and Pijaudier-Cabot, G. (1987). "Softening in reinforced concrete beams and frames." *J. Struct. Engrg.*, ASCE, 113(12), 2333–2347.

Bažant, Z. P., and Kazemi, M. T. (1988). "Determination of fracture energy, process zone length and brittleness number from size effect, with application to rock and concrete." *Report 88-7/498d*, Ctr. for Concr. and Geomatls., Northwestern Univ., Evanston, Ill., also *Intern. J. of Fracture*, in press.

Bažant, Z. P., and Pijaudier-Cabot, G. (1989). "Measurement of characteristic length of nonlocal continuum." *J. Engrg. Mech.*, ASCE, 115(4), 755–767.

Burt, N. J., and Dougill, J. W. (1977). "Progressive failure in a model heterogeneous medium." *J. Engrg. Mech. Div.*, ASCE, 103(3), 365–376.

Cundall, P. A. (1971). "A computer model for simulating progressive large scale movements in blocky rock systems." *Proc. Int. Symp. Rock Fracture*, ISRM, Nancy, France, 2–8.

Cundall, P. A. (1978). "BALL—A program to model granular media using the distinct element method." *Technical Note*, Advanced Tech. Grp., Dames and Moore, London, U.K.

Cundall, P. A., and Strack, O. D. L. (1979). "A discrete numerical model for granular assemblies." *Geotechnique*, 29, 47–65.

Kawai, T. (1980). "Some considerations on the finite element method." *Int. J. Numer. Meth. Engrg.*, 16, 81–120.

Owen, D. R. J., and Hinton, E. (1980). *Finite elements in plasticity: Theory and practice*. Pineridge Press Ltd., Swansea, U.K.

Plesha, M. E., and Aifantis, E. C. (1983). "On the modeling of rocks with microstructure." *Proc. 24th U.S. Symp. Rock Mech.*, Texas A&M Univ., College Station, Tex., 27–39.

Rodriguez-Ortiz, J. M. (1974). "Study of behavior of granular heterogeneous media by means of analogical mathematical discontinuous models." Thesis presented to the Universidad Politecnico de Madrid, at Madrid, Spain, in partial fulfillment of the requirements for the degree of Doctor of Philosophy (in Spanish).

Rots, J. G., Hordijk, D. A, and de Borst, R. (1987). "Numerical simulation of concrete fracture in direct tension." *Proc. 4th Int. Conf. on Numerical Methods in Fracture Mech.*, San Antonio, Tex., A. R. Luxmoore et al., eds., Pineridge Press, Swansea, U.K., 457–471.

Serrano, A. A., and Rodriguez-Ortiz, J. M. (1973). "A contribution to the mechanics of heterogeneous granular media." *Proc., Symp. Plasticity and Soil Mech.*, Cambridge, U.K.

Zubelewicz, A. (1980). "Contact element method." Thesis presented to The Technical University of Warsaw, at Warsaw, Poland, in partial fulfillment of the requirements for the degree of Doctor of Philosophy (in Polish).

Zubelewicz, A. (1983). "Proposal of a new structural model of concrete." *Archiwum Inzynierii Ladowej*, 29(4), 417–429 (in Polish).

Zubelewicz, A., and Bažant, Z. P. (1987). "Interface element modeling of fracture in aggregate composites." *J. Engrg. Mech.*, ASCE, 113(11), 1619–1630.

Zubelewicz, A., and Mróz, Z. (1983). "Numerical simulation of rockburst processes treated as problems of dynamic instability." *Rock Mech. and Engrg.*, 16, 253–274.